Seventh International Conference on
Computational Fluid Dynamics (ICCFD7),
Big Island, Hawaii, July 9-13, 2012

ICCFD7-2901

Simulation of Liquid Jet Breakup Process by Three-Dimensional Incompressible SPH Method

T. Takashima*, T. Ito**, M. Shigeta**, S. Izawa** and Y. Fukunishi**
Corresponding author: takashima@fluid.mech.tohoku.ac.jp

* Furukawa Electric Co., Ltd., Japan
** Tohoku University, Japan.

Abstract: The breakup processes of steady and pulsating jets are simulated using a three-dimensional incompressible SPH method. Experiments are also carried out and the results are compared. It is shown that the pinch-off length of a liquid jet depends on the Reynolds number. It oscillates at the same frequency as the pulsating jet. It is shown that the SPH can simulate these characteristics, though the pinch-off length tends to be longer when the jet velocity periodically changes with time.

Keywords: SPH, Surface Tension, Liquid Jet Breakup.

1 Introduction

A liquid jet breakup is well-known phenomena, which can be observed in our daily life. Water drops falling from a tap or the edge of an eave are the typical examples. When a high-speed liquid jet breaks up, a very fine mist is generated. This atomization process is widely used in various industrial applications such as ink-jet printings or fuel injections in internal combustion engines. However, the progress of atomization technology has depended on the knowledge of skilled engineers owing to the difficulty in carrying out experiments at such a very high-speed and small-scaled environment.

The study of a fundamental breakup phenomenon of a liquid jet began in Rayleigh[1], where an infinitely long liquid column injected into an air was analyzed. Many studies have been carried out experimentally and numerically in the last several decades[2]. In particular, the weight on the numerical approaches increased as the computer technology developed. Richards *et al.*[3, 4] simulated the breakup process of a liquid-liquid jet using the VOF method and the Continuous Surface Force (CSF) method and showed the good agreement with the experimental results. Ménard *et al.*[5] also simulated the atomization process of a high-speed liquid spray shed into an ambient gas using the Level Set method. Shinjo *et al.*[6] conducted Direct Numerical Simulation (DNS) with fine grid resolution, six billion grid points, to investigate the physical mechanisms from the liquid jet injection through the droplet formation.

In this paper, the applicability of grid-free numerical approach to this kind of problems is examined. Smoothed Particle Hydrodynamics (SPH) method used in this study is a popular method not only in the fluid engineering but also in the material engineering. Our group has already applied the SPH method to various types of flows including a moving boundary problem[7], a phase changing flow[8], a fluid-structure interaction[9] and a Magnetohydrodynamic (MHD) flow[10]. In this paper, a simple breakup process of liquid jets is simulated by the SPH method. An experiment is also conducted to validate the numerical results.

2 Computational Method

2.1 Incompressible SPH Method

Since an ordinary SPH method is intrinsically a compressible analytical method, the time step, based on the sound speed of the fluid and the particle size, should be taken very small. It leads to tough requirements in the computational time and storage. To overcome this problem, the density-homogenizing algorithm proposed in the previous studies[7, 8, 9, 10] is incorporated into the computation at every time-step after the particles move according to their inertia. The position of each particle is adjusted repeatedly until the densities at all particle positions become lower than ± 1 % from the mean density. Then, each particle velocity at the next time step is obtained using the particle's final position after the adjustment. Through this procedure, the incompressible fluid motion is approximately simulated. The treatment of external forces acting on particles is explained in the following sections.

2.2 Treatment of Viscosity

In the original SPH method, the artificial viscosity is widely introduced to ease the large, unphysical oscillations generated downstream of the shocks. In incompressible SPH, this artificial viscosity is not necessary. Instead, the viscosity effect is taken into account by the diffusion of momentum, which is analogous to the thermal conduction. Hence, the momentum diffusion equation of particle a with mass m is expressed as,

$$\left(\frac{\partial \boldsymbol{v}}{\partial t}\right)_a = \left\{\frac{1}{2\rho}\left[\nabla^2(\mu\boldsymbol{v}) + \mu\nabla^2\boldsymbol{v} - \boldsymbol{v}\nabla^2\mu\right]\right\}_a$$

$$= \sum_b \frac{m_b}{\rho_a\rho_b}(\mu_a + \mu_b)(\boldsymbol{v}_a - \boldsymbol{v}_b)\frac{\boldsymbol{r}_{ab}\cdot\nabla_a W_{ab}}{|\boldsymbol{r}_{ab}|^2} \qquad (\boldsymbol{r}_a \neq \boldsymbol{r}_b). \tag{1}$$

where ρ is the density, $\boldsymbol{v}$ is the velocity vector, $\boldsymbol{r}$ is the position vector and μ is the dynamic viscosity. $\nabla_a W_{ab}$ denote the gradient of kernel $W_a b$ taken with respect to $\boldsymbol{r}_a$. M4-spline kernel is used in terms of CPU time saving. Owing to the symmetric form of the equation of particles a and b, the linear momentum is exactly conserved. It should be noted that only the liquid particles' motions are computed and no effect from the ambient gas particles are taken into account in the computation.

2.3 Surface Tension Model

Surface tension plays a major role in a liquid jet breakup phenomenon. Several models were proposed to introduce the surface tension into the SPH method. Morris[11] used the Laplace pressure estimated from the interface curvature, while Nugent *et al.*[12] used attractive forces between particles. Hashimoto *et al.*[13] described the surface tension using the free energy theory[14].

In this study, the effect of surface tension is modeled as the Laplace pressure[15] as well as Morris[11]. The detailed procedures are as follows: First, the surface particles of liquid column are identified. If a particle is close to the surface, because the air particles are not existing, the weighted center of the surrounding particles shift inward away from the liquid surface. Using this characteristic, a surface particle can be identified as the particle whose distance between the weighted center and the particle position is longer than 25 % of the particle diameter. The reference density ρ_0 is assigned to these surface particles, because the density obtained as a summation of surrounding particles show a low value for surface particles because the air particles are absent. Next, the vectors normal to the surface at the surface particle positions are calculated and the surface curvature is obtained from the location where the normal vectors cross. This process in detail is:

1. Choose two planes crossing at right angles and project neighboring particles to these planes using the

weighted function $H(r)$,

$$H(r) = \cos\left(\frac{\pi r}{2h}\right) \qquad (|r| \leq h), \qquad (2)$$

where r is the distance from the plane.

2. Calculate the normal vectors at each position of surface particles and determine the radius of curvature R_{ai}.

3. Obtain the corresponding radii of curvatures R_1 and R_2 by taking their weighted averaging R_{ai}.

The Laplace pressure is calculated from these curvature radii R_1 and R_2,

$$P_{\mathrm{L}} = \gamma\left(\frac{1}{R_1} + \frac{1}{R_2}\right), \qquad (3)$$

where P_{L} is the Laplace pressure and γ is the surface tension coefficient.

3 Numerical Parameters and Experimental Setup

Figure 1 shows the initial particle distributions at $t = 0$ ms, and at certain time steps afterwards. A water jet is vertically ejected downwards at the Poiseuille velocity profile through a cylindrical nozzle of inner diameter d (= 3mm) and length l (= 4mm). Gravitational acceleration of 9.8 m/s^2 is given to all the liquid particles outside the nozzle. The diameter of a particle d_0 is 0.2 mm and fifteen particles are aligned each section inside the nozzle. Total numbers of particles of the water and the nozzle are 3,460 and 3,360, respectively, at the beginning of the computation. The axes of coordinate system are set as shown in the figure. The streamwise length between the breakup position and the nozzle end is denoted by L. The section-averaged outflow velocities at the nozzle end are set at $\bar{u} = 0.2$, 0.3, 0.38, 0.52, 0.61, 0.71, 1.08, 1.28, and 1,7 m/s. The kinetic viscosity and the surface tension coefficient are given as $\nu = 1.207{\times}10^{-6}$ m^2/s and $\gamma = 73.77{\times}10^{-3}$ N/m, respectively, which are the physical properties of a water at 13 °C.

In addition to steady jet, the pulsating jet is also simulated. The pulsation is given by the periodic change of the outflow velocity. The time variation of the outflow velocity is given as the sine wave function;

$$\bar{u}(t) = \bar{u}_{\mathrm{m}} + A_{\mathrm{m}}\sin(\frac{2\pi t}{T}), \qquad (4)$$

where $\bar{u}_{\mathrm{m}}$, A_{m}, and T are the time-averaged velocity, the amplitude, and the period, respectively. The pulsating period is $T = 50$ ms, or the pulse frequency is $F = 1/T = 20$ Hz. The mean velocity is $\bar{u}_{\mathrm{m}} = 0.39$ m/s. The values of T and $\bar{u}$ are the same as the experiment described later. Since the amplitude A_{m} could not be measured in the experiment, the pulsating liquid jet is simulated under the various amplitudes A_{m}, 0.05, 0.1, and 0.2 m/s. The kinetic viscosity and the surface tension coefficient are $\nu = 1.315{\times}10^{-6}$ m^2/s and $\gamma = 74.20{\times}10^{-3}$ N/m, which are the physical properties of a water at 10 °C.

Experiments are also carried out to validate the numerical results. Figure 2 shows the experimental setup for a steady jet. A tank filled with water has a hole of diameter 6 mm at its lower part of the sidewall. Water leaked through this hole finally flows out from the nozzle of inner diameter 3 mm, as shown the figure. To keep the water level constant, water overflows from the top of the tank. An averaged-discharge velocity $\bar{u}$ is measured from the flow rate. This velocity is set in the range of 0.2 m/s $\leq \bar{u} \leq$ 1.7 m/s by adjusting the valve. A thermometer is installed in the tank to monitor the temperature of the water and it is kept constant at $T_{\mathrm{w}} = 13$ °C. From this temperature, the kinetic viscosity ν and the surface tension coefficient γ are estimated as $1.207{\times}10^{-6}$ m^2/s and $73.77{\times}10^{-3}$ N/m, respectively. The behavior of the liquid jet ejected from the nozzle is tracked using a high-speed camera of the maximum 1,200 frames per second (fps).

In the experiment of the pulsating jet, the outflow velocity is controlled by a periodic deformation of the elastic tube at a location between the tank and the valve. An eccentric cylinder connected to a motor and a plate sliding up and down are used to deform the tube periodically. The pulsating period T is adjusted to be close to 50 ms, in other words the pulse frequency F is 20 Hz. The time-averaged outflow velocity is set at;
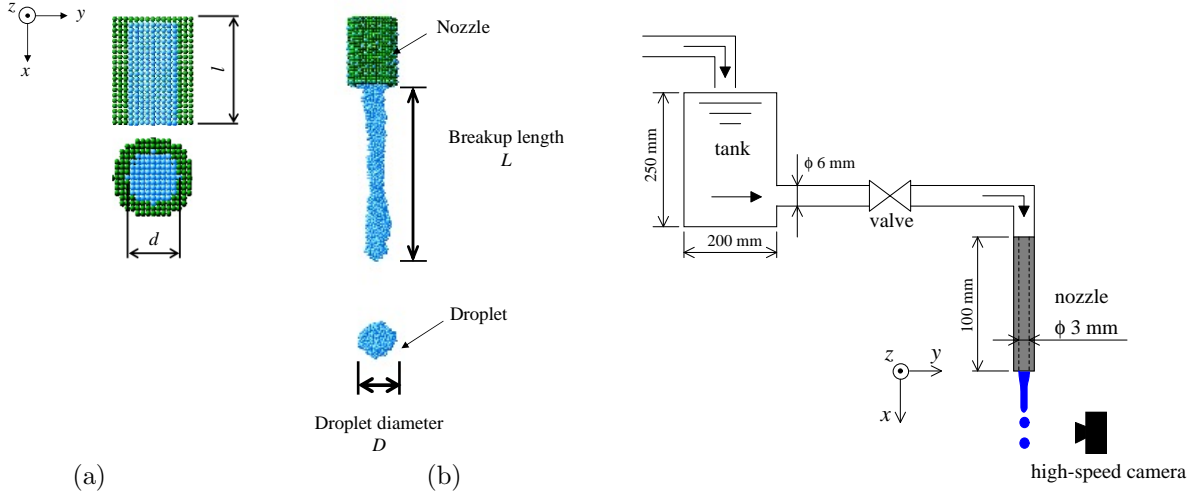
Figure 1: Particle distribution at (a) $t = 0$ ms and (b) after a certain time step.

Figure 2: Experimental setup for steady liquid jet.

(i) $t = 0$ ms   (ii) $t = 5$ ms   (iii) $t = 14.2$ ms
(a) Experiment.

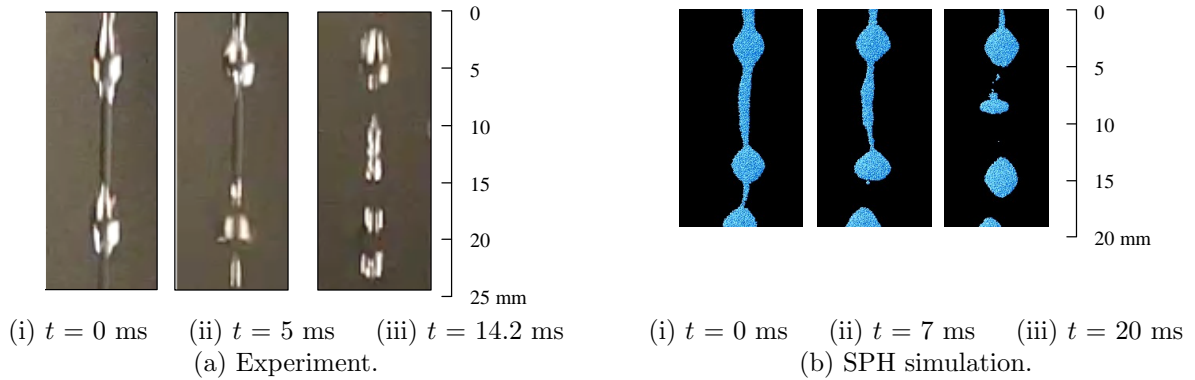(i) $t = 0$ ms   (ii) $t = 7$ ms   (iii) $t = 20$ ms
(b) SPH simulation.

Figure 3: Comparison of breakup processes at $Re = 944$ ($\bar{u} = 0.38$ m/s).

I). $\bar{u} = 0.42$ m/s when the sliding plate reaches the highest position and the tube is not deformed,

II). $\bar{u} = 0.41$ m/s when the tube is fully and constantly deformed by the plate, and

III). $\bar{u} = 0.39$ m/s when pulsating jet is generated.

The water temperature is kept constant at $T_{\mathrm{w}} = 10$ °C throughout the experiment.

4 Results and Discussion

The breakup process of a liquid column is investigated, focusing on the pinch-off length L which is the distance from the nozzle tip to the pinch-off position.

Figure 3 shows the comparison of breakup process between the experiment and the computation of a steady jet at $Re = 944$ ($\bar{u} = 0.38$ m/s). The moment when a liquid column starts to constrict is defined as $t = 0$ ms. Similar behaviors are observed in the experiment and numerical simulation, regarding the sizes, the gap lengths, and the liquid shapes. Once a constriction starts, the part becomes thinner and thinner as time advances. Finally, a lower part of the liquid column is pinched off and it soon becomes rounded owing to the surface tension. The intermediate drops[16] can be observed.

Figure 4 shows the variation of pinch-off length L for different Reynolds numbers $Re = \bar{u}d/\nu$. An error bar in this figure indicates the range of the standard deviation from the mean value. From the experimental results, the following tendency was observed:
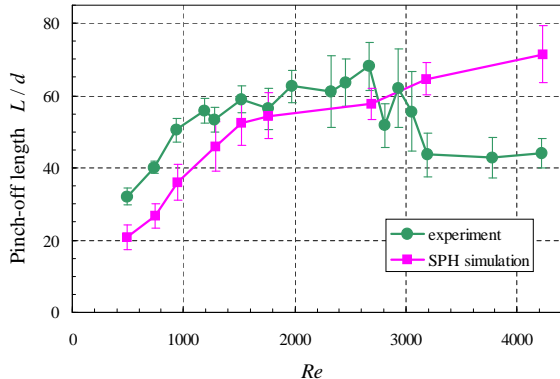
4

Figure 4: Comparison of pinch-off lengths.

Figure 5: Comparison of leading edge locations between experiment and SPH simulation at $\bar{u} = 0.39$ m/s (Re =890) and $A_m = 0.1$ m/s.

   I). $Re \leq 1{,}200$: The pinch-off length monotonously increases with outflow velocity.

  II). $1{,}200 < Re \leq 2{,}600$: Irregularity appears.

III). $2{,}600 < Re \leq 3{,}200$: The pinch-off length decreases randomly.

IV). $Re > 3{,}200$: The pinch-off length stays constant.

Tanasawa *et al.* also reported a similar tendency[16]. These results imply that the jet is laminar for $Re < 1{,}200$, turbulent at $Re > 3{,}200$, and otherwise in the transition region.

    In the simulation, the pinch-off length increases at $Re < 2{,}800$ as well as in the experiment, though it is smaller than the experimental results. The reason for the discrepancy in the pinch-off length is still unknown, a subject for the future studies. In contrast, the pinch-off lengths in the range $Re > 2{,}800$ are larger in the numerical results than those of the experiment. This discrepancy might be due to the numerical viscosity; however no remarkable change could be obtained regarding the pinch-off length even in a computation using ten-times the number of particles.

    Figure 5 shows comparison of the time variations of liquid column lengths H between experiment and SPH simulation at $\bar{u} = 0.39$ (Re =890) and $A_m = 0.1$ m/s. The origin $t = 0$ ms is an arbitrary value. The length of liquid columns periodically changes with time at a regular interval $t/T = 1$ s, which is equal to the forcing period. It is also found that the peak-to-peak difference of H in the numerical result is almost the same as that of the experiment: 14.4 in the simulation and 12.7 in the experiment, though its averaged value is more than twice of the experimental value.
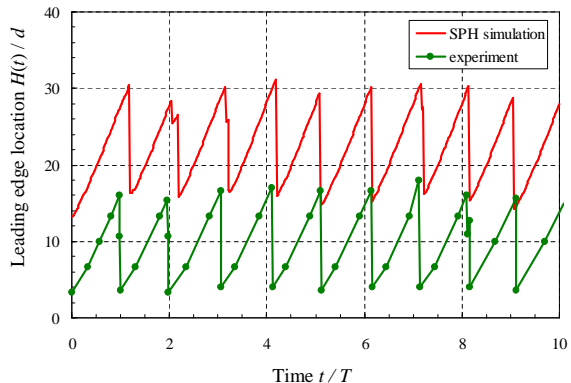
5 Conclusions

    Breakup process of a liquid jet ejected from a cylindrical nozzle was simulated using a three-dimensional incompressible SPH method under two different conditions: steady jet and pulsating jet. The numerical results agreed well with the experimental results, with the exception of the pinch-off length.

References

[1] F. R. S. Rayleigh. On the Instability of Jets. *Proc. London Math Soc.*, 10:4-13, 1878.

[2] J. Eggers and E. Villermaux. Physics of liquid jets. *Rep. Prog. Phys.*, 71:036601, 2008.

[3] J. R. Richards, A. M. Lenhoff and A. N. Beris. Dynamic breakup of liquid-liquid jets. *Phys. Fluids*, 6:2640-2655, 1994.

[4] J. R. Richards, A. N. Beris and A. M. Lenhoff. Drop formation in liquid-liquid systems before and after jetting. *Phys. Fluids*, 7:2617-2630, 1995.

[5] T. Ménard and S. Tanguy. Coupling level set/VOF/ghost fluid methods: Validation and application to 3D simulation of the primary break-up of a liquid jet. *Int. J. Multiphase Flow*, 33:510-524, 2007.

[6] J. Shinjo and A. Umemura. Simulation of liquid jet primary breakup: Dynamics of ligament and droplet formation. *Int. J. Multiphase Flow*, 36:513-532, 2010.

[7] T. Sano, S. Izawa, A. K. Xiong and Y. Fukunishi. The numerical simulation of flow which has free surface and deformation boundary by SPH method for incompressible fluid. *Proc. 83rd JSME Fluids Engineering Conference*, (2005-10), CD-ROM (in Japanese).

[8] M. Agawa, M. Shigeta, S. Izawa and Y. Fukunishi. Incompressible SPH Simulation of a Liquid Flowing down an Inclined Plane. *Proc. 23th Symposium on Computational Fluid Dynamics*, A9-4, 2009 (in Japanese).

[9] S. Tada, M. Satake, M. Shigeta, S. Izawa and Y. Fukunishi. Coupling Model of Incompressible Fluid and Elastic Structure by Three-dimensional SPH Method. *Proc. 25th Symposium on Computational Fluid Dynamics*, D05-1, 2011, (in Japanese).

[10] M. Shigeta, M. Ito, S. Izawa and Y. Fukunishi. Three-dimensional simulation of a flow in an arc weld pool by SPH method. *Transactions of JWRI*, 39(2):11-13, 2010.

[11] J. P. Morris. Simulating surface tension with smoothed particle hydrodynamics. *Int. J. Numer. Meth. Fluids*, 33:333-353, 2000.

[12] S. Nugent, H. A. Posch. Liquid drops and surface tension with smoothed particle applied mechanics. *Phys. Rev. E*, 62:4968-4975, 2000.

[13] Y. Hashimoto, Y. Yamaguchi, K. Kuroda, T. Nakajima and H. Fujimura. SPH Simulations of Binary Collision between Liquid Droplet with Different Surface Tension and Interfacial Tension. *Proc. 25th Symposium on Computational Fluid Dynamics*, E05-2, 2011 (in Japanese).

[14] D. M. Anderson and G. B. McFadden. Diffuse-Interface Methods in Fluid Mechanics. *Annu. Rev. Fluid Mech.*, 30:139-165, 1998.

[15] T. Hongo, M. Shigeta, S. Izawa and Y. Fukunishi. Modeling of Surface Tension Acting on Gas-Liquid Interface in Three-Dimensional Incompressible SPH Computation. *Proc. 23th Symposium on Computational Fluid Dynamics*, A8-5, 2009 (in Japanese).

[16] Y. Tanasawa and S. Toyoda. On the Atomization of Liquid Jet Issuing from a Cylindrical Nozzle. *Technol. Rep. Tohoku Univ.*, 19:135-156, 1955.